ACS Catalysis

RESEARCH ARTICLE

pubs.acs.org/acscatalysis

Polyhedral Oligomeric Silsesquioxane-Encapsulating Amorphous Palladium Nanoclusters as Catalysts for Heck Reactions

Chu-Hua Lu and Feng-Chih Chang*,†

†Institute of Applied Chemistry, National Chiao Tung University, 30010 Hsinchu, Taiwan

Supporting Information

ABSTRACT: Palladium nanoparticles (Pd NPs) capped with a certain protective group possessing stable reactivity of Pd-catalyzed reactions has been quickly and easily synthesized. The thiol−Pd^{2+} complexes of C_{12}−Pd^{2+} and POSS−Pd^{2+} are prepared by the ligand exchange of acetate groups on $Pd(OAc)_2$ with 1-dodecanthiol and SH-POSS (polyhedral oligomeric silsesquioxane), respectively. After thermal treatment at 120 °C for 30 min, the C_{12}−Pd^{2+} and POSS−Pd^{2+} turn into C_{12}−Pd(0) and POSS−Pd(0) NPs through the reduction of palladium cations with thiol groups. Unlike the well-known metallic Pd NPs with constituent Pd atoms arranged in an orderly repeating pattern, the cores of these thial−Pd(0) NPs are composed of a disordered (amorphous) aggregation of Pd atoms due to the steric hindrance caused by the affinity between in situ Pd atoms and thial groups. The relatively larger gaps between two adjacent POSS moieties, formed by solvent permeation when one isobutyl group approaches another, can be employed as transportation channels for reactants such as iodobenzene (IB). Thus, methyl *trans*-cinnamate is produced as soon as the reactants of IB and methyl acrylate are added in the POSS−Pd(0) NP-catalyzed Heck coupling. In contrast, an activation time of ∼1 h is needed for C_{12}−Pd(0) NPs to replace these long-alkyl protective groups with iodobenzene.

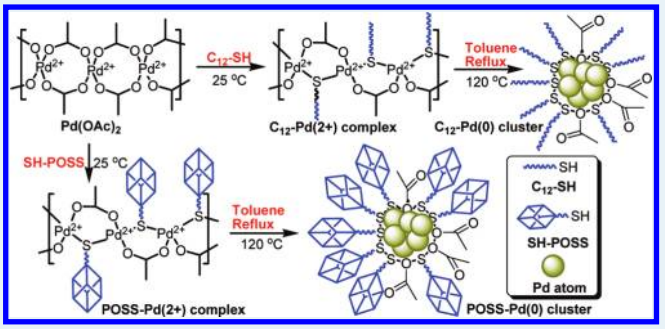

KEYWORDS: palladium nanoclusters, POSS, Heck coupling, catalyst

INTRODUCTION

Palladium nanoparticles (Pd NPs) are the most widely used transition-metal catalysts in modern organic synthesis, including Heck, Stille, Suzuki, Sonogashira, and Buchwald−Hartwig reactions.[1−5] However, the separation of the Pd NPs from the desired product, the stability to retain its activity, and the reusability often complicate their applications.[1] In this regard, many efforts have been made to immobilize Pd NPs onto a support (e.g., charcoal, silica, or alumina[6−9]), resulting in high catalytic activities, but the stability to Pd species' leaching is not satisfactory.[10] Alternatively, the encapsulation of Pd NPs by polymers[11−16] or dendrimers[17−19] has been reported, but these Pd NPs require further mechanical stabilization against leaching out or the breakage of the host.

Recently, a number of reports have been published on the immobilization of Pd NPs via ligand/polymer anchoring[20−22] and layer-by-layer assembly onto an organic solid support.[23] However, being a soft material, the ligand/polymer may not provide enough robustness against metal leaching or for recyclability.[24] In recent years, the ionic liquids and the related solid ionic liquid phase catalysis have been successfully used in Pd-catalyzed reactions.[25−27] In addition to the above-mentioned supported catalysts, de Vries et al. discovered that palladacycles such as cyclic trimer of Pd-$(OAc)_2$ can be directly used to catalyze a ligand-free Heck reaction.[28−30] In these studies, Pd^{2+} complexes and the product of Pd(0) NPs can be dispersed by iodide ions, which are converted from iodobenzene. Interestingly, ligand-free $Pd(OAc)_2$ palladacycles can be used as a catalyst in the Heck reaction of aryl bromides as long as the amount of catalyst is kept between 0.01 and 0.1 mol %. However, iodide ion is not a strong stabilizer for Pd(0) NPs so as to produce the low reactive precipitate of Pd black. Thus, a stable ligand is still necessary for the design of a recyclable catalyst.

Polyhedral oligosilsesquioxane (POSS), the cyclic oligomer of ladderlike poly(silsesquioxanes), consists of a 0.53-nm-diameter cubical siloxane core and eight organic short arms stretched from the corners of the core.[31] In organic solution, POSS can be regarded as a molecular colloid with soluble organic groups to disperse an inorganic core by steric stabilization.[32] Similar to other structurally symmetrical molecules, POSS colloids can be stacked up into ordered structures (colloidal crystals) after removal of solvent, with evidence of low-angle-diffraction signals shown in the wide-angle X-ray scattering (WAXS) patterns. In our previous study,[33] we found the specific arrangement of alkyl POSS molecules in a crystal. Like a metal crystal, alkyl POSS has a hexagonal unit cell with a dimensional ratio c/a of 1.06. This value is much lower than the expected 1.63 for a hard-sphere, closed-packing mode. Considering the size of alkyl POSS, we concluded that there are small cavities in an alkyl POSS crystal that are occupied by solvent molecules. This result can be attributed to the fact that POSS molecules tend to absorb solvent

Received: September 23, 2010
Published: March 15, 2011

Scheme 1. Synthesis of C_{12}−Pd and POSS−Pd Amorphous Nanoclusters

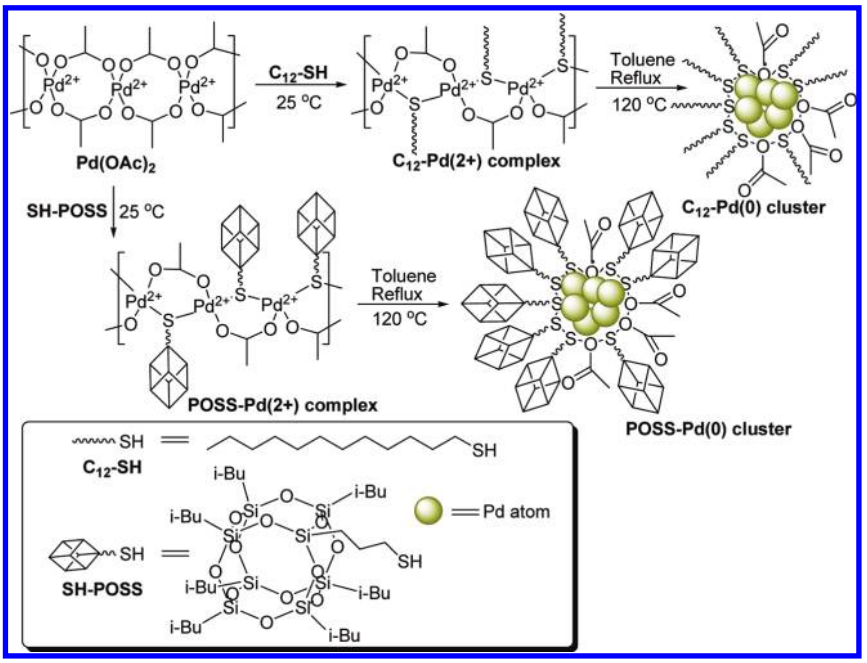

molecules to separate each other. Consequently, thiol-functional POSS (SH-POSS) not only would be an excellent ligand to stabilize a metal NP but also provides channels for transport reactants and products for reactions on the surface of metal NPs.[31−38] In addition, the thiol groups are often incorporated onto mesoporous silica particles because of the strong affinity of thiol to Pd^{2+} ions and Pd(0) NPs.[39,40]

Typically, there are four raw materials—metal salts, reductants, stabilizer, and phase-transfer agents—that are required for the chemical synthesis of metal NPs. Using a hydrophobic stabilizer, a phase-transfer agent is usually required to cover the water-soluble metal salts, and then they are transferred into the organic phase. Different from hydrophilic metal salts, the palladium acetate $[Pd(OAc)_2]$ is a source of Pd salts that can be dissolved in many organic solvents (e.g., toluene, tetrahydrofuran, methanol) because of its cyclic trimer $[Pd_3(\mu\text{-}O_2CMe)_6]$ capped with organic acetate ligand.[41,42] Relative to other water-soluble Pd salts, such as palladium chloride ($PdCl_2$) and disodium tetrachloropalladate (Na_2PdCl_4),[43−46] $Pd(OAc)_2$ was therefore adopted for the preparation of Pd NPs in a single phase without phase-transferring agents. In addition to chemical reductants (e.g., $NaBH_4$),[47−51] most Pd NPs are prepared from Pd salts using solvent reductants (e.g., alcohols,[52−54] phosphines,[55−59] and amines[55−59]) that are capable of reducing Pd salts by self-oxidizing. According to the periodic table, thiol may also be expected to serve as a reductive solvent because sulfur (thiol) exists in the same group as oxygen (alcohol) and the same period as phosphorus (phosphine). However, to the best of our knowledge, no reports mentioned this concept. Therefore, we are motivated to study the thiol-mediated reduction of $Pd(OAc)_2$ with SH-POSS or C_{12}−SH in the synthetic procedure shown in Scheme 1.

RESULTS AND DISCUSSION

Thiol−Pd^{2+} Complexes. Two thiol−Pd^{2+} complexes, C_{12}−Pd^{2+}, and POSS−Pd^{2+} complexes, were prepared by dissolving

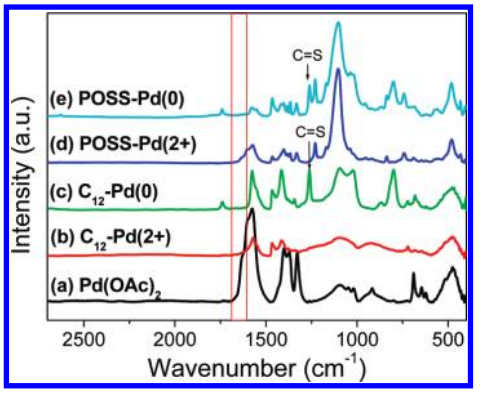

Figure 1. FTIR spectra of (a) $Pd(OAc)_2$, (b) C_{12}−Pd^{2+} complexes, (c) C_{12}−Pd(0) NPs, (d) POSS−Pd^{2+} complexes, and (e) POSS−Pd(0) NPs.

$Pd(OAc)_2$ (0.11 g, 0.5 mmol) and 1-dodecanthiol (SH−C_{12}, 0.10 g, 0.5 mmol) or 3-mercaptopropyl isobutyl polyhedral oligomeric silsesquioxane (SH-POSS, 0.45 g, 0.5 mmol) in argon-purged toluene (20 mL). The reaction mechanisms are shown in Scheme 1. In the previous study on thiol−Pd^{2+} complexes, Basato et al. reported that the cyclic trimer of $Pd(OAc)_2$, $Pd_3(\mu\text{-}O_2CMe)_6$, can react with 2 equiv of $HSCH_2C(O)Me$ to produce the full-sulfur-ligand complex $[Pd(SCH_2C(O)Me)_2]_3$.[42] Although thiols can be efficiently substituted for all acetate groups, the equimolar quantities of $Pd(OAc)_2$ and thiol ligands, such as C_{12}−SH and SH-POSS are considered sufficient to provide a thiol monolayer for the colloidal stabilization of 1−5-nm-diameter Pd NPs in solution. The equivalent feed ratio of $Pd(OAc)_2$ to thiols (mol/mol) was used, and then the formation of partially thiol-substituted Pd^{2+} complexes was characterized by Fourier transform infrared (FTIR) spectroscopy, ultraviolet−visible (UV−vis) spectroscopy, and WAXS patterns.

dx.doi.org/10.1021/cs200106s |ACS Catal. 2011, 1, 481–488

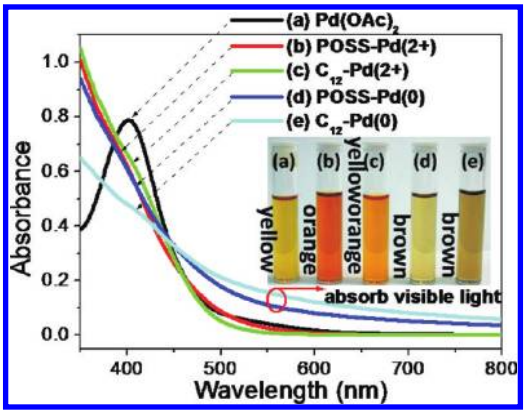

Figure 2. UV−vis spectra of (a) $Pd(OAc)_2$, (b) POSS−Pd^{2+} complexes, (c) C_{12}−Pd^{2+} complexes, (d) POSS−Pd(0) NPs, and (e) C_{12}−Pd(0) NPs.

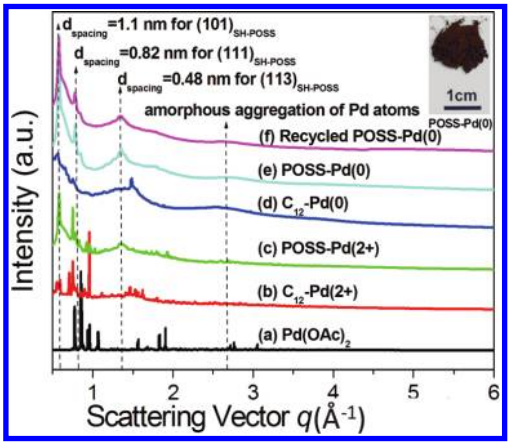

Figure 3. WAXS patterns of (a) $Pd(OAc)_2$, (b) C_{12}−Pd^{2+} complexes, (c) POSS−Pd^{2+} complexes, (d) C_{12}−Pd(0) NPs, (e) POSS−Pd(0) NPs, and (f) recycled POSS−Pd(0) NPs.

The color of the $Pd(OAc)_2$ solution changes from yellow to orange upon mixing with the C_{12}−SH or SH-POSS (see the insert of Figure 2). This color change coupled with the following FTIR and UV−vis studies support the formation of the thiol−Pd^{2+} complex. As shown in Figure 1a, the FTIR spectrum of $Pd(OAc)_2$ displays two peaks at 1633.8 and 1601.4 cm^{-1}, representing the C−O stretching modes of the metal-bonded μ-acetate ion. By contrast, these two peaks weaken when the $Pd(OAc)_2$ is blended with equimolar C_{12}−SH or SH-POSS in toluene (red square in Figure 1b and d), providing evidence to support the release of low-vapor-pressure acetic acid for the formation of thiol−Pd^{2+} complexes (Scheme 1).[41,42,60−64]

A similar approach was reported previously by Kim et al. in the investigation of the release of acetylacetone from the blend of palladium acetylacetone and trioctylphosphine through FTIR detecting a C═C stretching peak at 1630 cm^{-1} (enol form of acetylacetone).[55] As for the UV−vis characterizations, the color shifts of the solution in UV−Vis absorbances also reveal the characteristics of metal complexes with distinct ligands. The yellow solution of $Pd(OAc)_2$ in toluene featuring a visible light absorbance at 402 nm (Figure 2a) shifts to lower wavelengths (<350 nm) and tails off in the visible region (~550 nm), resulting in orange and yellow/orange solutions of POSS−Pd^{2+} and

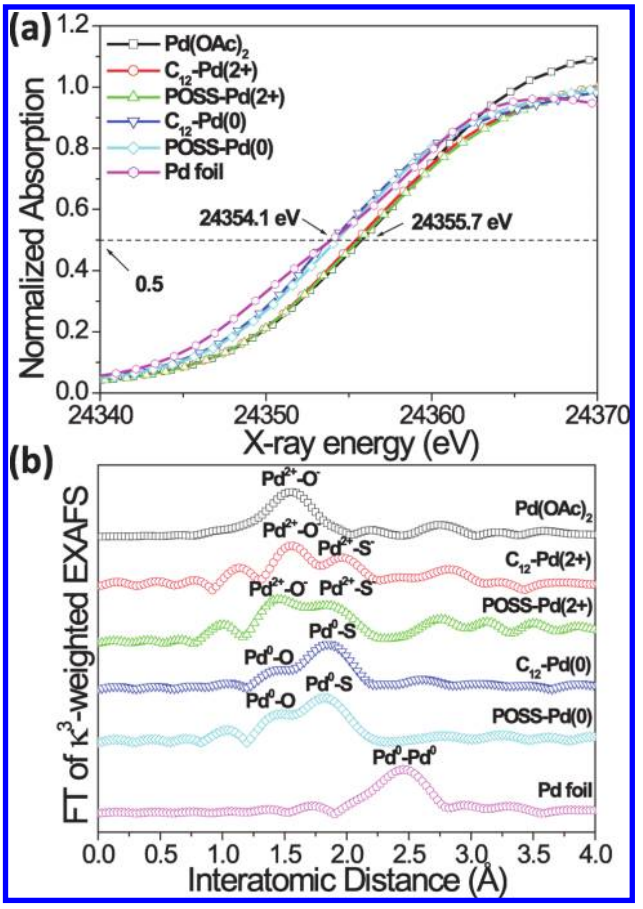

Figure 4. (a) Pd K-edge XANES spectra and (b) Fourier transforms of κ^3-weighted Pd K-edge EXAFS spectra of $Pd(OAc)_2$, C_{12}−Pd^{2+} complexes, POSS−Pd^{2+} complexes, C_{12}−Pd(0) NPs, POSS−Pd(0) NPs, and standard Pd foil.

C_{12}−Pd^{2+} complexes by blending with equimolar SH-POSS or C_{12}−SH (Figures 2b and 2c).[60] In adition, in comparison with an ionic crystal of $Pd(OAc)_2$ (Figure 3a),[41,42,65] the WAXS signals of the thiol−Pd^{2+} complexes at high scattering vectors ($q > 1$) disappear in Figure 3b and c, an indication of amorphous packing of Pd atoms, probably due to the inhibition of crystallization using the long alkyl chain thiol (C_{12}−SH) or the bulky siloxane cube thiol (SH-POSS).[60−64] The C_{12}−Pd^{2+} complex is a nonmobile liquid at 25 °C; the POSS−Pd^{2+} complex is a powder at 25 °C, featuring crystallization of the POSS moieties according to the three signals of a POSS crystal for the diffraction planes of (101), (111), and (113) (Figure 3c).[33]

Thial−Pd(0) Clusters. Similar to the amine-mediated reduction of amine−Au(3+) complexes,[66] the thiol-mediated reduction of the thiol−Pd^{2+} complexes generates dark colloidal thial−Pd(0) nanoclusters solutions in toluene under reflux (~120 °C) for 30 min. This redox procedure, the combination of the reduction of Pd^{2+} complexes into Pd(0) clusters and the oxidation of thiol anions (RCH_2S^-) to thials (RCH═S), is achieved by the ligand-to-metal charge transfer from S^- (π electrons) to Pd^{2+} (4d orbital).[52−54] As shown by FTIR spectra, Figure 1c and e indicate the C═S stretching at 1256 cm^{-1} which is not intense and falls at lower wavenumbers because the C═S group is less polar than the C═O group.[67]

The significant features of the bulky, hydrophobic, and symmetrical POSS molecules tend to crystallize in methanol. These

dx.doi.org/10.1021/cs200106s |ACS Catal. 2011, 1, 481–488

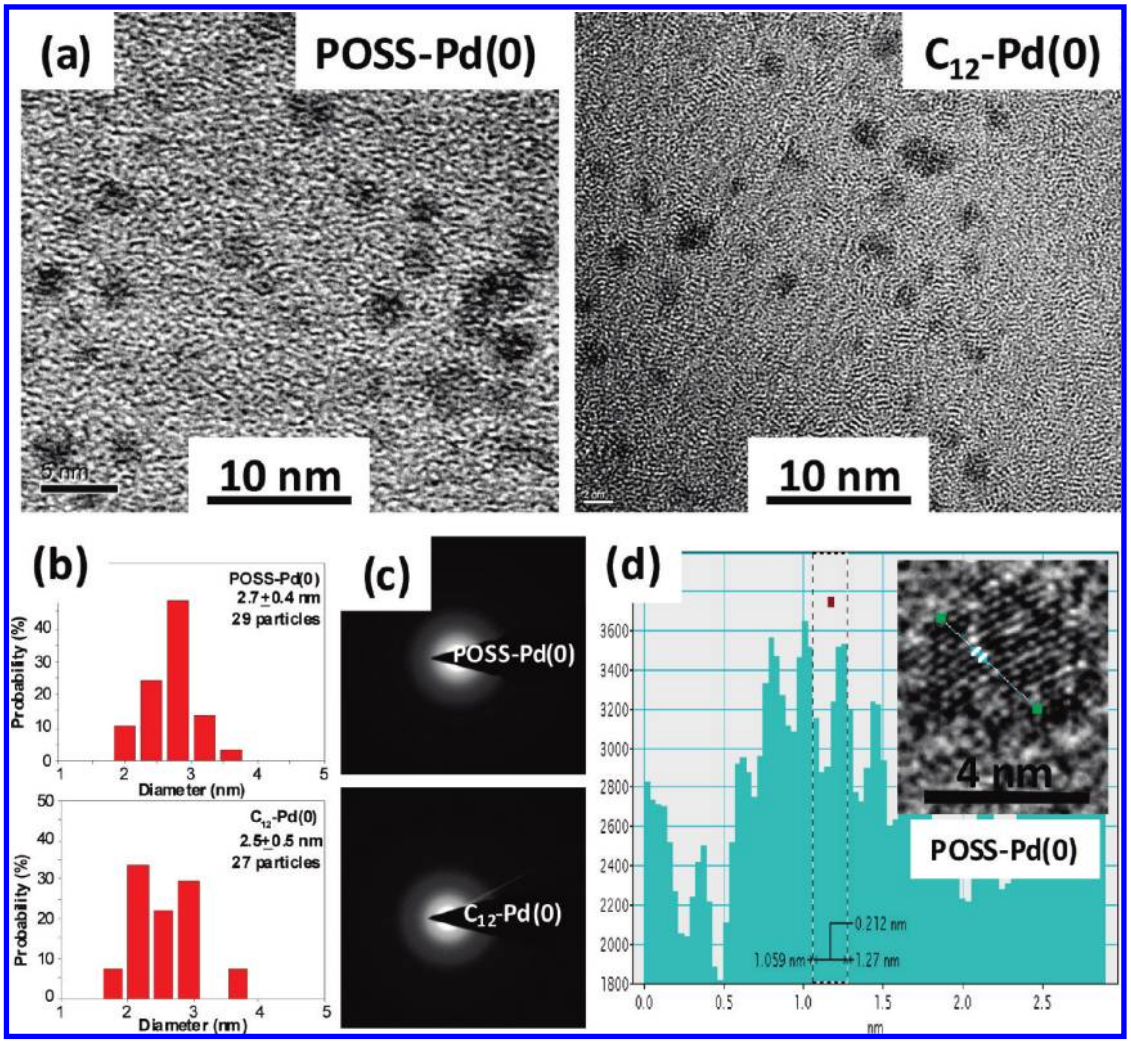

Figure 5. (a) Bright-field images, (b) size distribution histogram, (c) electron diffraction patterns of the C_{12}−Pd(0) and POSS−Pd(0) NPs, and (d) the atomic lattice fringe of the POSS−Pd(0) NPs.

POSS-capped metal NPs are able to be arranged into a complex solid with the connection of excess POSS crystals; nevertheless, the crystallization of metal-bonded POSS molecules is inhibited. Thus, the yields of 76 and 82% for C_{12}−Pd(0) and POSS−Pd(0) NPs (inset to Figure 3) are obtained after purification by precipitation of thial−Pd(0) clusters in MeOH.[43−46] These precipitates are readily redispersed in nonpolar organic solvents (i.e., toluene) to give homogeneous dark brown solutions. The dilute brown solutions of the POSS−Pd(0) and C_{12}−Pd(0) clusters feature their UV−vis absorbances (400−800 nm) of the well-known surface plasmon resonances (Figure 2d and e).[54,68−70] Unlike metallic Pd nanocrystals in the previous reports,[52−54,68−70] the cores of the as-synthesized thial-Pd(0) clusters are amorphous, based on the observation of one broad amorphous peak (q) at 2.7 $Å^{-1}$ in the WAXS patterns of the C_{12}−Pd(0) and POSS−Pd(0) NPs (Figure 3d and e), corresponding to the disordered aggregation of Pd atoms. Nevertheless, such a broad signal of WAXS spectra for metal NPs can be attributed to their small sizes. Therefore, the further and direct proof of this finding is performed by X-ray absorption spectroscopy (XAS) and transmission electron microscopy (TEM).

XAS Spectra. XAS is a powerful and generally applicable spectroscopic tool that provides element-specific information regarding the atomic and electronic structure of molecular species. Here, we compare XAS spectra of thiol−Pd^{2+} complexes, thial−Pd(0) clusters, $Pd(OAc)_2$, and a Pd foil. Figure 4a shows the Pd K-edge spectra of X-ray absorption near-edge structures (XANES) of $Pd(OAc)_2$ and a Pd foil, indicating the midpoints of normalized K-edge energies of Pd(0) at 24 354.1 eV and Pd^{2+} at 24 355.7 eV, respectively.[71] The midpoint of normalized K-edge energy is very important to judge the oxidation state because it tends to shift to higher energy with the increased oxidation state.[71−76] Comparatively, the midpoints of normalized K-edge energies of the thiol−Pd^{2+} complexes are similar to $Pd(OAc)_2$, whereas the thial−Pd(0) clusters shift to the same position as a Pd foil (Figure 4a). In addition, Figure 4b displays the Fourier transforms of the κ^3-weighted extended X-ray absorption fine structure (EXAFS) at the Pd K-edge.

The main peaks from $Pd(OAc)_2$ and Pd foil are located around 1.54 and 2.47 Å (without phase correction), which can be attributed to the adjacent oxygen (Pd−O) and palladium (Pd−Pd) atoms, respectively. To compare with $Pd(OAc)_2$, the Pd−O intensity for the C_{12}−Pd^{2+} complex at 1.55 Å decreases while the Pd−S intensity at 1.97 Å appears, indicating that the acetate anions are replaced by thiols (Scheme 1). For the POSS−Pd^{2+} complex, the peaks of Pd−O and Pd−S shift toward

dx.doi.org/10.1021/cs200106s |*ACS Catal.* 2011, 1, 481–488

shorter distances of 1.43 and 1.89 Å, probably due to the slightly distorted conformation of the bulk and partially sulfur−ligand complex of $[Pd_3(\mu\text{-}O_2CMe)_3(S\text{-}POSS)_3]$ (Scheme 1).[77]

After the thiol-mediated reduction, this steric effect on the structural conformation is diminished by ring-opening of the cyclic structure of $[Pd_3(\mu\text{-}O_2CMe)_6]$, and then, Pd atoms aggregate into an amorphous NPs, with the evidence of the similar Pd−O and Pd−S signals at 1.42 and 1.83 Å for C_{12}−Pd(0) and POSS−Pd(0) NPs. Herein, C_{12}−Pd(0) and POSS−Pd(0) are similar to $Pd(PPh_3)_4$, having a palladium atom surrounded by bulky ligands. The shifts observed in the XANES spectra clearly suggest that the thiol-mediated reduction is achieved through the transformation from the thiol−Pd^{2+} complexes into thial−Pd(0) NPs (Figure 4a). The crystallization of Pd atoms is inhibited by Pd−S bonds and thus results in amorphous Pd(0) NPs.[62,63,74,78]

TEM Analysis. TEM is a typically applicable microscopic technique that renders the element-contrastive images at a significantly higher resolution than optic microscopies. Figure 5a and b displays bright-field TEM images and size distribution of the POSS−Pd(0) and C_{12}−Pd(0) NPs, indicating the average sizes of 2.7 ± 0.4 and 2.5 ± 0.5 nm for POSS−Pd(0) and C_{12}−Pd(0) NPs, respectively. POSS−Pd NPs have been reported.[79−82] They used water-soluble octa(tetramethylammonium)-polyhedral oligomeric silsesquioxane as an anionic ligand to disperse Pd cations and stabilize Pd NPs. However, POSS−Pd NPs tend to aggregate through the ionic interaction.

In this study, the POSS−Pd(0) NPs using SH-POSS can be dispersed in toluene, and their dispersion can be observed by TEM images in Figure 5a. The broad halos in the electron diffraction patterns of the C_{12}−Pd(0) and POSS−Pd(0) NPs correspond to the amorphous aggregation Pd atoms (Figure 5c), and these results are consistent with those from WAXS (Figure 3d and e) and XAS (Figure 4b) analyses. When the high-energy electron beam is transmitting through samples at the high magnification of TEM images, the local heating can induce the recrystallization of amorphous NPs into metallic NPs so that atomic lattice fringes with a regular layer-to-layer distance of 0.212 nm are observed for a 4-nm-diameter POSS−Pd(0) amorphous nanocluster (Figure 5d).[83,84] Although these atomic lattice fringes are produced by local heating, they can confirm that the dark spots in the TEM images are composed of Pd atoms. As reported by Kim et al,[55,85−87] the Pd atoms can recrystallize at 300 °C to provide the more uniform size and the higher crystallinity of Pd NPs. The amorphous thial−Pd(0) NPs are considered to possess high catalytic reactivity to Heck coupling because of the lower energy barrier to release Pd atoms in the step of oxidative addition with IB (Scheme 2b). Thus, we used the thial−Pd(0) nanoclusters directly, without further aging, to test their applicability in Heck couplings.[79−82,88−93]

Pd(0)-Catalyzed Heck Coupling. Heck reaction is the most powerful and widely used for coupling of alkenes with organic moieties bearing a suitable leaving group (e.g., halide, triflate, or diazonium). The Heck coupling of IB and MA has been frequently used as a model reaction (Scheme 2a) to study new Pd catalysts.[88−93] This transformation follows four steps (Scheme 2b): oxidative addition, π-complexation, insertion/β-hydride elimination, and reductive elimination.[1−5] Herein, the Heck couplings of IB and MA are performed in *N*-methylpyrrolidone (NMP) to give methyl *trans*-cinnamate (MC) by using POSS−Pd(0) and C_{12}−Pd(0) NPs (Figure 6a).[83,84] In addition, the tributylamine (TBA) is employed to trap the side product of HI

Scheme 2. (a) Reaction Scheme and (b) Mechanism for the Heck Coupling of MA and IB To Give MC

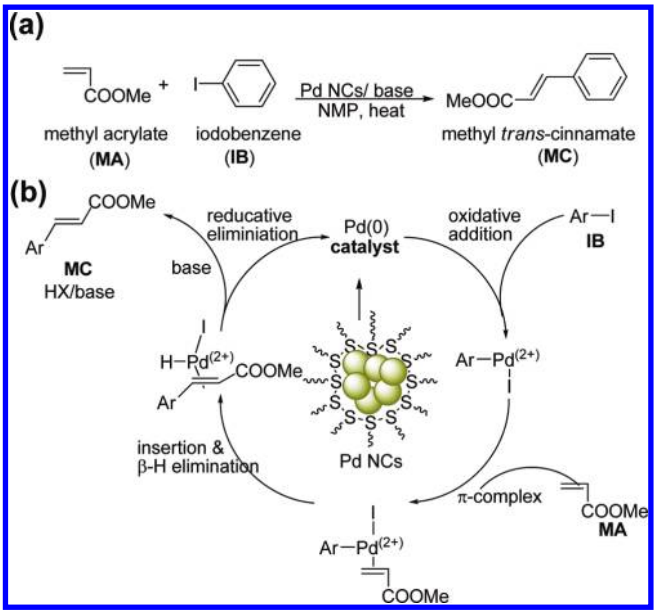

in the form of an ammonium salt, and these Heck reactions are performed at 75 °C due to low-boiling-point MA (T_b∼ 80 °C).

Although GC/MS analysis is typically used, we found it is more convenient to qualitatively and quantitatively determine the conversions of MA by the vinyl protons H_b and H_g in ^{1}H NMR spectra (Figure 6a).[84] Using POSS−Pd(0) and C_{12}−Pd(0) NPs, the MC is produced in 100% selectivity; i.e., no cis form is shown in the ^{1}H NMR spectra (Figure 6a). After 6 h, the conversions of MA reach at least 99.7% (Figure 6b). Note that using the C_{12}−Pd(0) NPs, the Heck coupling requires an additional 1 h of activation time, probably resulting from the exchanging thials for IB.[90] Comparatively, using the POSS−Pd(0) NPs, the reaction occurs as soon as the reactants are mixed, because the wider gaps between the bulk and thiol-functional POSS provide molecular channels for transportation of IB.

According to Figure 6b, the slopes of time−conversion profiles are 62.6 and 24.8% h^{-1} for Heck reactions of 5 mmol MA using 0.128 mmol Pd of POSS−Pd(0) and C_{12}−Pd(0) NPs, respectively. Hence, the turnover frequencies are 24.45 and 9.69 mol reactant × mol Pd^{1-} h^{-1}, respectively.[94] Theoretically, the first-order reaction rate is proportional to the concentrations of the reactants. If the catalyst does not require activation or deactivation during Heck coupling, the rate constant will be constant. Thus, time−$\ln([M]_0/[M])$ curves should be linear after mathematical integration. Figure 6b displays time−conversion and time−$\ln([M]_0/[M])$ curves for the POSS−Pd(0) and C_{12}−Pd(0) NPs. The line of the time−$\ln([M]_0/[M])$ plot with a slope of 1.52 s^{-1} indicates the excellent catalytic stability of the POSS−Pd(0) NPs, and thus, the decay at high MA conversions is simply attributed to the low concentrations of the reactants. In comparison, the S curve in the time−$\ln([M]_0/[M])$ plot for the C_{12}−Pd(0) NPs suggests a complicated mechanism involving activation and deactivation.

As mentioned above, high-molar-mass hydrophobic POSS-protected Pd NPs are easily purified by precipitating in MeOH.[43−46] Therefore, we can easily recycle the POSS−Pd NPs. The thermogravity analyses (onset points and char yields at

dx.doi.org/10.1021/cs200106s |*ACS Catal.* 2011, 1, 481–488

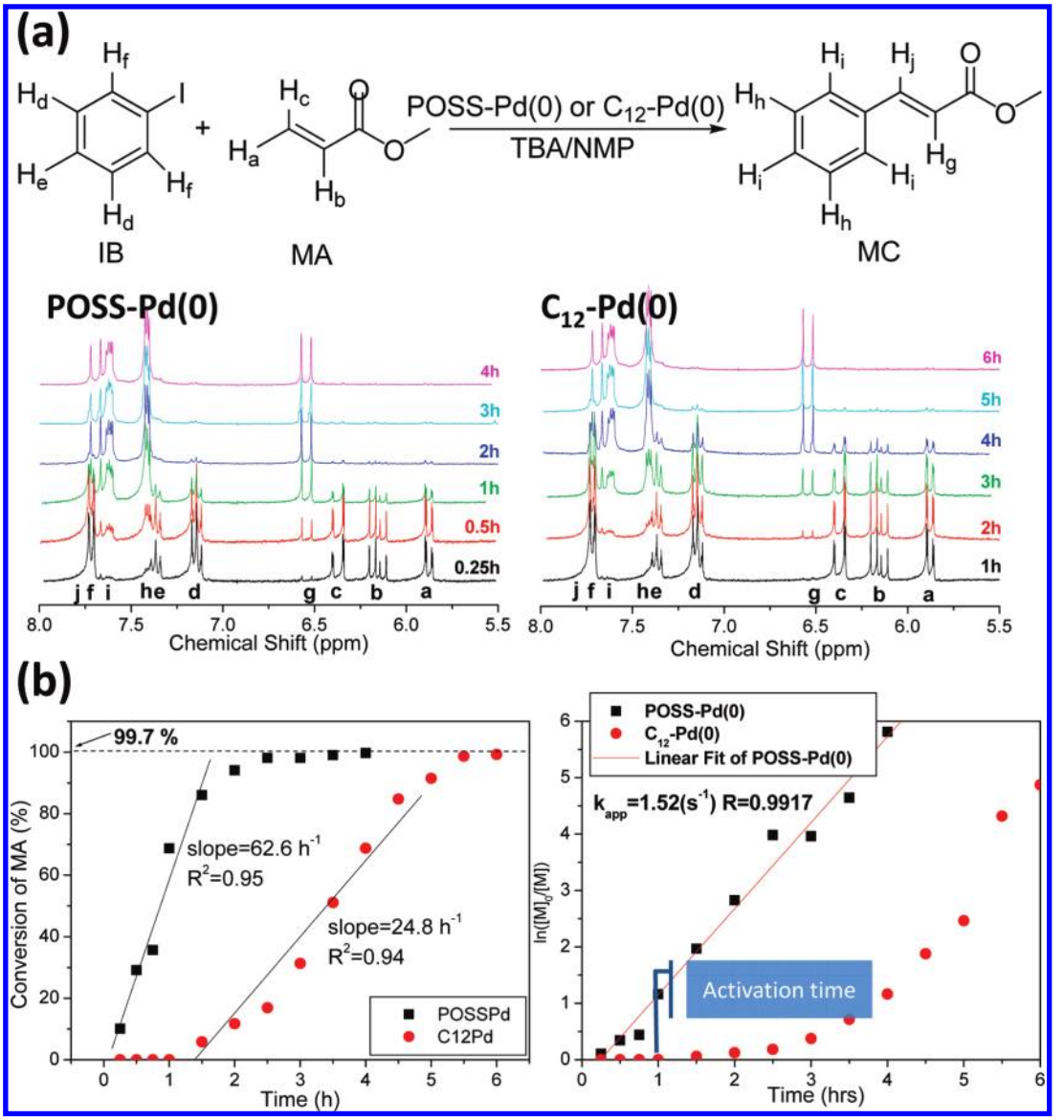

Figure 6. (A) ^{1}H NMR spectra of reaction mixture and (B) time−conversion and time−ln([M]$_0$/[M]) profiles of Heck reactions using catalysts of POSS−Pd(0) and C_{12}−Pd(0) NPs. Reaction conditions: 75 °C; catalysts, 0.1 g POSS−Pd(0) or 0.035 g C_{12}−Pd(0) NPs (including 0.128 mmol Pd); NMP, 30 mL; iodobenzene and methyl acrylate, 5 mmol each; tributylamine, 7.5 mmol.

700 °C in the Supporting Information) and the WAXS patterns (Figure 3e and f) indicate that the as-synthesized and the recycled POSS−Pd(0) NPs have similar composition and structure; that is, the POSS moieties are not repelled from the recycled POSS−Pd(0) NPs (see the Supporting Information).[33−35] However, the recycling yields of Pd NPs are about 50 wt % in each cycle when either the as-synthesized or the recycled POSS−Pd(0) NPs are used.[83,84] This is because the structures of remaining Pd species (i.e., tributyl ammonium iodide-capped metallic Pd NPs, in the filtrate (MeOH−filtrate POSS−Pd)) are different from those of the as-synthesized or the recycled POSS−Pd(0) NPs with POSS-capped amorphous Pd NPs (see evidence in the Supporting Information). Interestingly, the catalytic reactivity of the MeOH−filtrate POSS−Pd can be retained in at least four cycles of reuse by adding another charge of IB, MA, and TBA at 75 °C for another 4 h. Nevertheless, discussion of the catalytic characteristic of MeOH−filtrate POSS−Pd is beyond the scope of this paper. Regarding MeOH−filtrate POSS−Pd, future work will hopefully clarify this important catalytic concern.

CONCLUSIONS

Similar to those methods by using reductive solvents (e.g., alcohols, amines, and phosphines), the thiols such as SH-POSS and C_{12}−SH can be used for the preparation of Pd NPs such as POSS−Pd(0) and C_{12}−Pd(0) in toluene under reflux (~120 °C) for 30 min, respectively. In this approach, the thiols can be served simultaneously as reductants and protective groups in the preparation of Pd NPs. The products of C_{12}−Pd(0) and POSS−Pd(0) NPs are different from the well-known metallic Pd NPs because their cores are composed of disordered aggregation of Pd atoms due to the affinity between Pd atoms and thial groups. The POSS−Pd NPs function as excellent and nanosized

dx.doi.org/10.1021/cs200106s |*ACS Catal.* 2011, 1, 481–488

storage vessels of Pd atoms when employed in the Heck coupling of iodobenzene and methyl acrylate at 75 °C to form methyl *trans*-cinnamate. The results show first-order reaction of POSS−Pd(0) NP-catalyzed Heck coupling without activation or deactivation of Pd active sites because the wider gaps between bulk POSSs render transportation channels for the input of IB.

■ ASSOCIATED CONTENT

Supporting Information. Additional information as noted in text. This material is available free of charge via the Internet at http://pubs.acs.org.

■ AUTHOR INFORMATION

Corresponding Author
*E-mail: changfc@mail.nctu.edu.tw.

■ ACKNOWLEDGMENT

This study was supported in part by the National Science Council under the Grant NSC97-2120-M-009-003. We thank the National Synchrotron Radiation Research Center of Taiwan for technical support during the recording of the X-ray absorbance (BL01C1) and wide-angle X-ray scattering (BL01C2).

■ REFERENCES

(1) Yin, L.; Liebscher, J. *Chem. Rev.* **2007**, *107*, 133–173.
(2) Li, J. J.; Gribble, G. W. *Palladium in Heterocyclic Chemistry*; Pergamon: Amsterdam, 2000.
(3) Amatore, C.; Jutand, A. *Acc. Chem. Res.* **2000**, *33*, 314–321.
(4) Choudary, B. M.; Madhi, S.; Kantam, M. L.; Sreedhar, B.; Iwasawa, Y. *J. Am. Chem. Soc.* **2004**, *126*, 2292–2293.
(5) Malleron, J.-L.; Fiaud, J.-C.; Legros, J.-Y. In *Handbook of Palladium-Catalyzed Organic Reactions*; Academic Press: London, 2000.
(6) Marck, G.; Villiger, A.; Buchecker, R. *Tetrahedron Lett.* **1994**, *35*, 3277–3280.
(7) LeBlond, C. R.; Andrews, A. T.; Sun, Y.; Sowa, J. R., Jr. *Org. Lett.* **2001**, *3*, 1555–1557.
(8) Choudary, B. M.; Madhi, S.; Chowdari, N. S.; Kantam, M. L.; Sreedhar, B. *J. Am. Chem. Soc.* **2002**, *124*, 14127–14136.
(9) Patel, A. C.; Li, S.; Wang, C.; Zhang, W.; Wei, Y. *Chem. Mater.* **2007**, *19*, 1231–1238.
(10) Raja, R.; Khimyak, T.; Thomas, J. M.; Herman, S.; Johnson, B. F. G. *Angew. Chem., Int. Ed.* **2001**, *40*, 4638–4642.
(11) Akiyama, R.; Kobayashi, S. *Angew. Chem., Int. Ed.* **2001**, *40*, 3469–3471.
(12) Jansson, A. M.; Groti, M.; Halkes, K. M.; Meldal, M. *Org. Lett.* **2002**, *4*, 27–30.
(13) Ramarao, C.; Ley, S. V.; Smith, S. C.; Shirley, I. M.; DeAlmeida, N. *Chem. Commun.* **2002**, 1132–1133.
(14) Lee, C. K. Y.; Holmes, A. B.; Ley, S. V.; McConvey, I. F.; Al-Duri, B.; Leeke, G. A.; Santos, R. C. D.; Seville, J. P. K. *Chem. Commun.* **2005**, 2175–2177.
(15) Okamoto, K.; Akiyama, R.; Yoshida, H.; Yoshida, T.; Kobayashi, S. *J. Am. Chem. Soc.* **2005**, *127*, 2125–2135.
(16) Oyamada, H.; Akiyama, R.; Hagio, H.; Naito, T.; Kobayashi, S. *Chem. Commun.* **2006**, 4297–4299.
(17) Crooks, R. M.; Zhao, M.; Sun, L.; Chechik, V.; Yeung, L. K. *Acc. Chem. Res.* **2001**, *34*, 181–190.
(18) Gopidas, R.; Whitesell, J. K.; Fox, M. A. *Nano Lett.* **2003**, *3*, 1757–1760.
(19) Ornelas, C.; Salmon, L.; Aranzaes, J. R.; Astruc, D. *Chem. Commun.* **2007**, 4946–4948.
(20) Hou, Z.; Theyssen, N.; Brinkmann, A.; Leitner, W. *Angew. Chem., Int. Ed.* **2005**, *44*, 1346–1349.
(21) Pathak, S.; Greci, M. T.; Kwong, R. C.; Mercado, K.; Prakash, G. K. S.; Olah, G. A.; Thompson, M. E. *Chem. Mater.* **2000**, *12*, 1985–1989.
(22) Shin, J. Y.; Lee, B. S.; Jung, Y.; Kim, S. J.; Lee, S. *Chem. Commun.* **2007**, 5238–5240.
(23) Kidambi, S.; Dai, J.; Li, J.; Bruening, M. L. *J. Am. Chem. Soc.* **2004**, *126*, 2658–2659.
(24) Li, Y.; El-Sayed, M. A. *J. Phys. Chem. B* **2001**, *105*, 8938–8943.
(25) Gu, Y.; Li, G. *Adv. Synth. Catal.* **2009**, *351*, 817–847.
(26) Welton, T. *Chem. Rev.* **1999**, *99*, 2071–2084.
(27) Cassol, C. C.; Umpierre, A. P.; Machado, G.; Wolke, S. I.; Dupont, J. *J. Am. Chem. Soc.* **2005**, *127*, 3298–3299.
(28) de Vries, J. G. *Dalton Trans* **2006**, 421–429.
(29) de Vries, A. H. M.; Mulders, J. M. C. A.; Mommers, J. H. M.; Henderickx, H. J. W.; de Vries, J. G. *Org. Lett.* **2003**, *5*, 3285–3288.
(30) Tucker, C. E.; de Vries, J. G. *Top. Catal.* **2002**, *19*, 111–118.
(31) Sheen, Y. C.; Lu, C. H.; Huang, C. F.; Kuo, S. W.; Chang, F. C. *Polymer* **2008**, *49*, 4017–4024.
(32) Romero-Cano, M. S.; Puertas, A. M.; de las Nieves, F. J. *J. Chem. Phys.* **2000**, *112*, 8654–8659.
(33) Lu, C.-H.; Kuo, S.-W.; Huang, C.-F.; Chang, F.-C. *J. Phys. Chem. C* **2009**, *113*, 3517–3524.
(34) Liu, L.; Tian, M.; Zhang, W.; Zhang, L.; Mark, J. E. *Polymer* **2007**, *48*, 3201–3212.
(35) Mantz, R. A.; Jones, P. F.; Chaffee, K. P.; Lichtenhan, J. D.; Gilman, J. W.; Ismail, I. M. K.; Burmeister, M. J. *Chem. Mater.* **1996**, *8*, 1250–1259.
(36) Naka, K.; Itoh, H.; Chujo, Y. *Bull. Chem. Soc. Jpn.* **2006**, *77*, 1767–1770.
(37) Carroll, J. B.; Frankamp, B. L.; Srivastava, S.; Rotello, V. M. *J. Mater. Chem.* **2004**, *14*, 690–694.
(38) Carroll, J. B.; Frankamp, B. L.; Rotello, V. M. *Chem. Commun.* **2002**, *17*, 1892–1893.
(39) Purcar, V.; Donescu, D.; Petcu, C.; Luque, R.; Macquarrie, D. J. *Catal. Commun.* **2009**, *10*, 395–400.
(40) Richardson, J. M.; Jones, C. W. *J. Catal.* **2007**, *251*, 80–93.
(41) Skapski, A. C.; Smart, M. L. *J. Chem. Soc. D* **1970**, 658–659.
(42) Basato, M.; Tommasi, D.; Zecca, M. *J. Organomet. Chem.* **1998**, *571*, 115–121.
(43) Şen, F.; Gökağaç, G. *J. Phys. Chem. C* **2007**, *111*, 1467–1473.
(44) Brust, M.; Walker, M.; Bethell, D.; Schiffrin, D. J.; Whyman, R. *J. Chem. Soc., Chem. Commun.* **1994**, 801–802.
(45) Li, Y.; Wu, Y.; Ong, B. S. *J. Am. Chem. Soc.* **2005**, *127*, 3266–3267.
(46) Cheng, Z.; Zhang, L.; Zhu, X.; Kang, E. T.; Neoh, K. G. *J. Polym. Sci., Polym. Chem.* **2008**, *46*, 2119–2131.
(47) Mastalir, Á.; Rác, B.; Király, Z.; Tasi, G.; Molnár, Á. *Catal. Commun.* **2008**, *9*, 762–768.
(48) Hou, W.; Dehm, N. A.; Scott, R. W. J. *J. Catal.* **2008**, *253*, 22–27.
(49) Wei, G.; Zhang, W.; Wen, F.; Wang, Y.; Zhang, M. *J. Phys. Chem. C* **2008**, *112*, 10827–10832.
(50) Li, F.; Bertoncello, P.; Ciani, I.; Mantovani, G.; Unwin, P. R. *Adv. Funct. Mater.* **2008**, *18*, 1685–1693.
(51) Ouiros, I.; Yamada, M.; Kubo, K.; Mizutani, J.; Kurihara, M.; Nishihara, H. *Langmuir* **2002**, *18*, 1413–1418.
(52) Li, D.; Dunlap, J. R.; Zhao, B. *Langmuir* **2008**, *24*, 5911–5918.
(53) Budarin, V. L.; Clark, J. H.; Luque, R.; Macquarrie, D. J.; White, R. J. *Green Chem.* **2008**, *10*, 382–387.
(54) Teranishi, T.; Miyake, M. *Chem. Mater.* **1998**, *10*, 594–600.
(55) Kim, S. W.; Park, J.; Jang, Y.; Chung, Y.; Hwang, S.; Hyeon, T. *Nano Lett.* **2003**, *3*, 1289–1291.
(56) Hyeon, T.; Lee, S. S.; Park, J.; Chung, Y.; Na, H. B. *J. Am. Chem. Soc.* **2001**, *123*, 12798–12801.
(57) Hyeon, T.; Chung, Y.; Park, J.; Lee, S. S.; Kim, Y.-W.; Park, B. H. *J. Phys. Chem. B* **2002**, *106*, 6831–6833.

(58) Joo, J.; Yu, T.; Kim, Y.-W.; Park, H. M.; Wu, F.; Zhang, J. Z.; Hyeon, T. *J. Am. Chem. Soc.* **2003**, *125*, 6553–6557.
(59) Burton, P. D.; Lavenson, D.; Johnson, M.; Gorm, D.; Karim, A. M.; Conant, T.; Datye, A. K.; Hernandez-Sanchez, B. A.; Boyle, T. J. *Top Catal.* **2008**, *49*, 227–232.
(60) Chauhan, B. P. S.; Rathore, J.; Sardar, R.; Tewari, P.; Latif, U. *J. Organomet. Chem.* **2003**, *686*, 24–31.
(61) Basato, M.; Bertani, C.; Sesto, B.; Zecca, M.; Grassi, A.; Valle, G. *J. Organomet. Chem.* **1998**, *552*, 277–283.
(62) Shimizu, K.; Koizumi, S.; Hatamachi, T.; Yoshida, H.; Komai, S.; Kodama, T.; Kitayama, Y. *J. Catal.* **2004**, *228*, 141–145.
(63) Shimizu, K.; Maruyama, R.; Komai, S.; Kodama, T.; Kitayama, Y. *J. Catal.* **2004**, *227*, 202–209.
(64) Sugiura, C.; Kitamura, M.; Muramatsu, S. *J. Chem. Phys.* **1986**, *85*, 5269–5272.
(65) Kirik, S. D.; Mulagaleev, R. F.; Blokhin, A. I. *Acta Crystallogr.* **2004**, *C60*, M449–M450.
(66) Hiramatsu, H.; Osterloh, F. E. *Chem. Mater.* **2004**, *16*, 2509–2511.
(67) Silverstein, R. M.; Webster, F. X. In *Spectrometric Identification of Organic Compounds*, 6th ed.; John Wiley and Sons: New York, 1997; p 106.
(68) Chen, D.; Zheng, L.-Z. *Chin. J. Chem.* **2008**, *26*, 276–280.
(69) Zhang, Q.; Xie, J.; Yang, J.; Lee, J. Y. *ACS Nano* **2009**, *3*, 139–148.
(70) Xiong, Y.; Chen, J.; Wiley, B.; Xia, Y.; Yin, Y.; Li, Z.-Y. *Nano Lett.* **2005**, *5*, 1237–1242.
(71) McCaulley, J. A. *Phys. Rev. B* **1993**, *47*, 4873–4879.
(72) de Groot, F. *Chem. Rev.* **2001**, *101*, 1779–1808.
(73) Westre, T. E.; Kennepohl, P.; Dewit, J. G.; Hedman, B.; Hodgson, K. O.; Solomon, E. I. *J. Am. Chem. Soc.* **1997**, *119*, 6297–6314.
(74) Bae, I. T.; Tryk, D. A.; Scherson, D. A. *J. Phys. Chem. B* **1998**, *102*, 4114–4117.
(75) Ramallo-López, J. M.; Giovanetti, L.; Craievich, A. F.; Vicentin, F. C.; Marín-Almazo, M.; José-Yacaman, M.; Requejo, F. G. *Physica B* **2007**, *389*, 150–154.
(76) Cho, S. J.; Kang, S. K. *Catal. Today* **2004**, *93*−*95*, 561–566.
(77) Xiang, H.; Kang, J.; Wei, S.-H.; Kim, Y.-H.; Curtis, C.; Blake, D. *J. Am. Chem. Soc.* **2009**, *131*, 8522–8526.
(78) Ooe, M.; Murata, M.; Mizugaki, T.; Ebitani, K.; Kaneda, K. *J. Am. Chem. Soc.* **2004**, *126*, 1604–1605.
(79) Aiken, J. D., III; Finke, R. G. *J. Mol. Catal. A: Chem.* **1999**, *145*, 1–44.
(80) Bonnemann, H.; Richards, R. M. *Eur. J. Inorg. Chem.* **2001**, 2455–2480.
(81) Roucoux, A.; Schulz, J.; Patin, H. *Chem. Rev.* **2002**, *102*, 3757–3778.
(82) Rozenberg, B. A.; Tenne, R. *Prog. Polym. Sci.* **2008**, *33*, 40–112.
(83) Biffis, A.; Zecca, M.; Basato, M. *J. Mol. Catal. A: Chem.* **2001**, *173*, 249–274.
(84) Biffis, A.; Zecca, M.; Basato, M. *Eur. J. Inorg. Chem.* **2001**, 1131–1133.
(85) Warren, S. C.; Banholzer, M. J.; Slaughter, L. S.; Giannelis, E. P.; DiSalvo, F. J.; Wiesner, U. B. *J. Am. Chem. Soc.* **2006**, *128*, 12074–12075.
(86) Lai, C.; Guo, Q.; Wu, X.-F.; Reneker, D. H; Hou, H. *Nanotechnology* **2008**, *19*, 195303–195310.
(87) Chen, L.; Hong, S.; Zhou, X.; Zhou, Z.; Hou, H. *Catal. Commnun.* **2008**, *9*, 2221–2225.
(88) Barau, A.; Budarin, V.; Caragheorgheopol, A.; Luque, R.; Macquarrie, D. J.; Prelle, A.; Teodorescu, V. S.; Zaharescu, M. *Catal. Lett.* **2008**, *124*, 204–214.
(89) Ambulgekar, G. V.; Bhanage, B. M.; Samant, S. D. *Tetrahedron Lett.* **2005**, *46*, 2483–2485.
(90) Zhao, F.; Bhanage, B. M.; Shirai, M.; Arai, M. *Chem.—Eur. J.* **2000**, *6*, 843–848.
(91) Zheng, P.; Zhang, W. *J. Catal.* **2007**, *250*, 324–330.
(92) Papp, A.; Galbacs, G.; Molnar, A. *Tetrahedron Lett.* **2005**, *46*, 7725–7728.
(93) Molnar, A.; Papp, A.; Mirlos, K.; Forgo, P. *Chem. Commum.* **2003**, 2626–2627.
(94) Garcia-Martinez, J. C.; Lezutekong, R.; Crooks, R. M. *J. Am. Chem. Soc.* **2005**, *127*, 5097–5103.